

Development and characterization of wax molds for 3D microfluidic applications

Rex Garland, Jonah Kohen, Fengjiao Lyu
Advisors: David Huber, Michelle Rincon, Caitlin Chapin

Abstract

The purpose of this project was to explore the uses of the 3D wax printer for rapid prototyping in a nanofabrication setting: where the time to design is roughly equal to the time to fabrication. As a motivating example, we use the wax printer to print truly 3D molds for microfluidic components in PDMS. We report the design and fabrication of a sheath flow component used for aligning blood cells in the center of a channel. We characterize the performance of the tools and materials we use, including detailed procedures for replicating our results.

Introduction

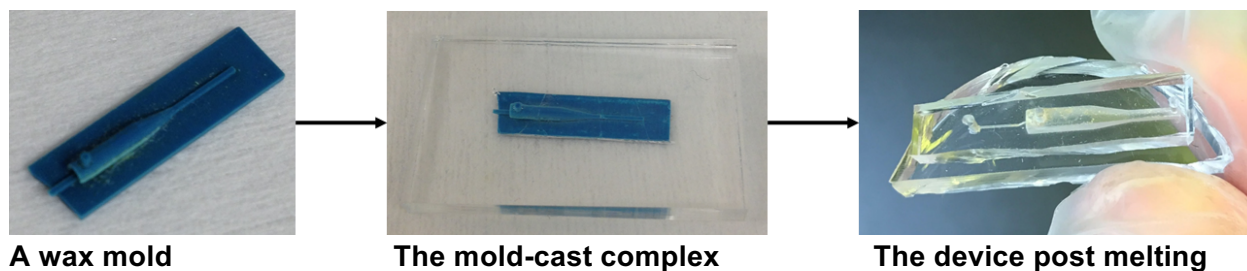
Conventional microfluidic devices are often created using 2D lithography. These devices can reach a minimum feature size of about 5 μm and take around a week to design and fabricate. Although this method is precise and repeatable in the context of microfluidics, the 2D nature of these devices limits their microfluidic uses. Creating valves, for example, requires another layer of 2D microfluidics. This is often called “2D+” [1] and involves stacking multiple lithographically fabricated microfluidic channels and interfacing them with vias. These devices are not truly 3D and often cannot achieve a vertical resolution on the scale of their lateral resolution. In order to create this level of 3D precision, a variety of techniques is available. One tool for creating 3D microfluidics is laser-induced curing of PDMS [2]. While this achieves high resolution, it is expensive and time-consuming. The same goes for two-photon 3D photoresists for creating molds. 3D printing techniques are more desirable because they are cheaper and can be done quickly using commercially available machines. While most 3D printers cannot achieve the resolution necessary to create microfluidic molds, 3D wax printers can achieve nominal vertical layers of about 6 μm . In this report we examine the advantages of using a wax printer and characterize its limits for use in microfabrication. We apply our findings to create a 3D sheath flow device for focusing fluids laterally and vertically. While conventional sheath flow involves 2D+ structures whereby sheath fluid focuses a central fluid in the vertical and horizontal direction, these geometries involve focusing in two steps and fluid becomes slightly less focused during each step (i.e. vertical focusing will spread out horizontal focusing). By creating a device which focuses in both dimensions simultaneously, the focusing power can be dramatically increased. We use a 3D-printed wax mold to create such a device, report its performance and suggest future iterations.

Problem Statement

The Solidscape 3ZStudio 3D wax printer is ideally suited to the problem of 3D printing microfluidic channels because it can create a variety of geometries at high resolution and create

a mold which can be melted at a low temperature (~100 °C). For our application, the wax printer was used to construct inverted microfluidic molds. The wax printer builds molds using two material types: support wax (red) and a low-temperature thermoplastic (blue) for creating the model. The support material encases every feature of the mold, allowing delicate structures to be fashioned without breaking. This allows for thin, suspended channels to be created, as required for three-dimensional sheath flow. This support wax can be dissolved in a mineral oil bath heated to its melting point. This step will be referred to as post-processing in this report.

Once the molds are created and post processed properly, PDMS, epoxy, or any other material we choose can be poured onto the wax mold. This material seeps around the structure and covers all features, thus forming the channel. Once the PDMS/epoxy/etc cures, its melting point will be far higher than the melting point of the build material, which Solidscape publishes to be between 95 and 110 degrees Celsius. Placing the cast-mold complex in an oven heated to the required melting point removes the wax and leaves the 3D microfluidic structure intact. The main steps in this process are shown below:



In order to generalize our work to that of other ExFab users, we characterized the performance of the wax printer for a variety of tests. This information and detailed instructions will be published on the Stanford Nanofabrication Facility wiki and are recorded here in the appendix.

Wax Printer Characterization

Solidscape Studio Capabilities	Nominal Capabilities	Measured Capabilities
Z-axis layer	~6 um	~14 um
Minimum feature size	250um	200um
Droplet size	76 um	~150um
Surface Roughness	0.9-1.6 um	0.6-1.2 um
X-Y positioning	197 dots/mm (~5um)	
Approximate Print Rate (including setup, auto-calibration)		5 min/mm³ (very slow)

Table 1: Comparison of commercially reported and experimentally measured wax printer capabilities. This table summarizes our major findings from characterization.

Screening test

A screening test was performed to quickly identify the approximate limits of the printer. One major error we noticed during this print was that residue remained on the print after post-processing. This residue appeared light blue when dry and darker when still submerged in mineral oil. The residue is most likely due to a powder formed during the print: build material accumulates in a dust form during printing and the printer uses a vacuum pump to remove this dust. However, if there are small features and sharp corners in the print itself and its surrounding support material, this dust can get stuck on the print regardless of the vacuum clean. The remaining dust might have lingered on the print and absorbed mineral oil, making it difficult to evaporate away with compressed air. Another challenge we ran into after this first characterization print was the strength of higher aspect ratio structures.

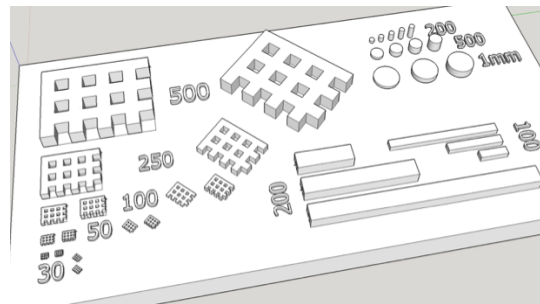


Figure 1: CAD model for screening test. Various grid sizes, heights, and orientations were printed. Cylinders of various aspect ratios were also printed. Channels were printed to test the ability to remove long crevices of support wax, but a better test was developed later (see well test below).

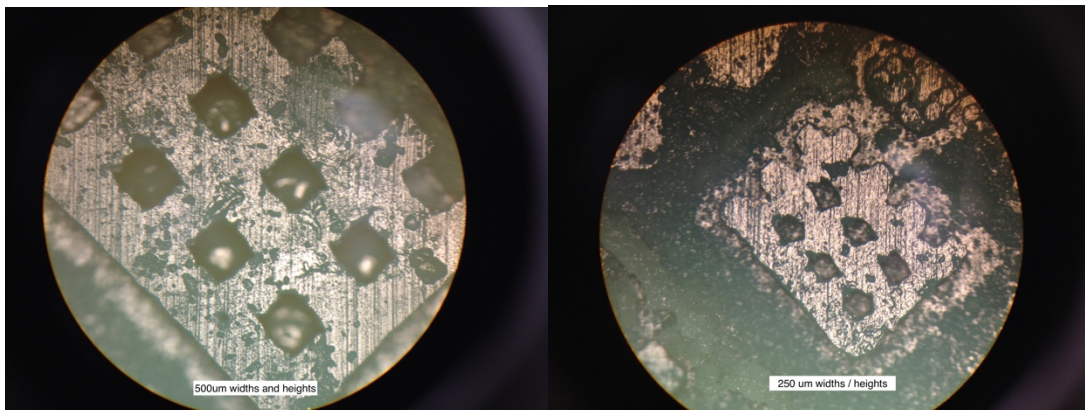


Figure 2 Optical images of a screening test characterization print. Grids printed at a 45 degree angle with respect to the rastering axes were similar in quality to those aligned with the rastering axes of the printer. Grids started to lose their definition around 250 μm channel widths.

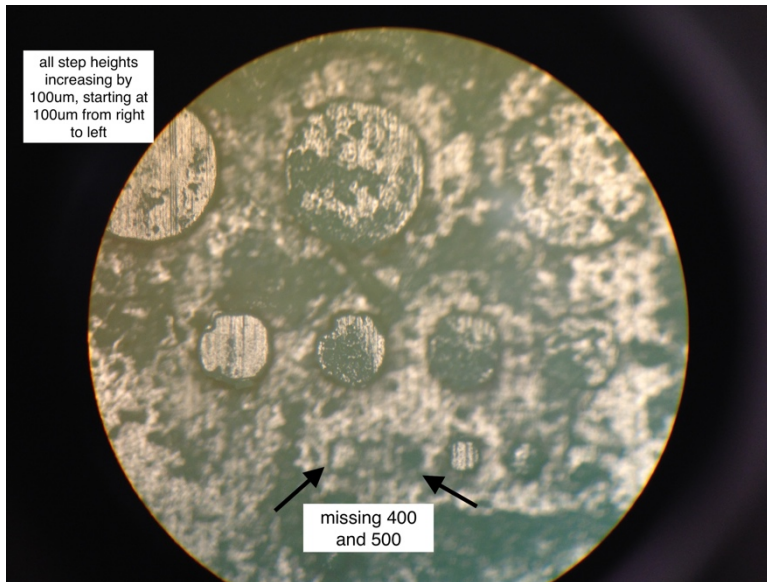


Figure 3: Optical image of cylinders printed during the screening test. Agitation (moving prints out of mineral oil bath, handling during characterization) causes structures with aspect ratio > 2 to break.

During characterization it appeared that pillars of a certain height were less smooth than others. A surface roughness test disproved this hypothesis (see below).

Surface Roughness V.S. Height

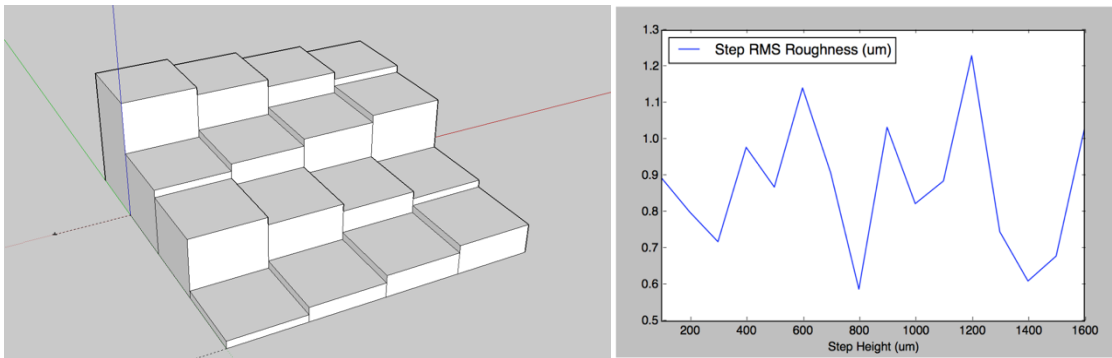
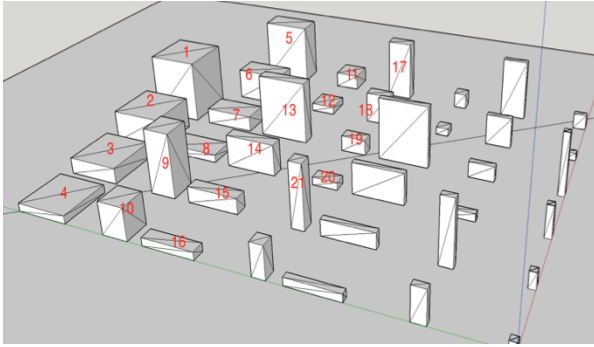


Figure 4: Step characterization test. Steps of various heights were printed to measure the change in surface roughness as a function of print height. Optical confocal profilometry showed that roughness and vertical position are uncorrelated.

Aspect Ratio Tests

While the surface properties of the prints were well within the ~5 μm resolution necessary for microfluidics, the ability to print small feature sizes depends on the structural stability and print accuracy of high aspect ratio features. We tested a variety of prisms with different aspect ratios see how precisely they would print.



		5 0.4, 0.8, 0.8	11 0.4, 0.4, 0.2	17 0.2, 0.4, 0.8
		6 0.4, 0.8, 0.4	12 0.4, 0.4, 0.1	18 0.2, 0.4, 0.4
1 0.8, 0.8, 0.8	7 0.4, 0.8, 0.2	13 0.2, 0.8, 0.8	19 0.2, 0.4, 0.2	
2 0.8, 0.8, 0.4	8 0.4, 0.8, 0.1	14 0.2, 0.8, 0.4	20 0.2, 0.4, 0.1	
3 0.8, 0.8, 0.2	9 0.4, 0.4, 0.8	15 0.2, 0.8, 0.2	21 0.2, 0.2, 0.8	
4 0.8, 0.8, 0.1	10 0.4, 0.4, 0.4	16 0.2, 0.8, 0.1		

Figure 5: CAD model and dimensions of aspect ratio characterization print. Only the indexed structures successfully printed. Indices are shown in red and mm dimensions (length, width, height) are shown in blue.

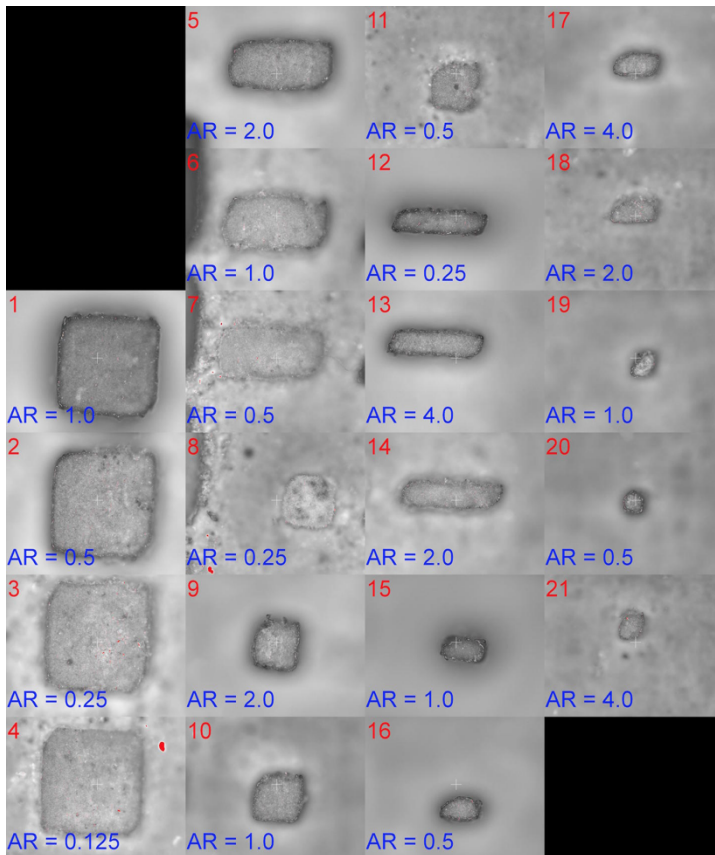


Figure 6: Optical images of the tops of aspect ratio characterization structures. Images are all on the same scale and the aspect ratio (AR) is shown for each. The fidelity of this top layer seems to depend less on the aspect ratio than it does on the minimum feature size.

No structures below 100 μm printed. The quality of each prism seemed to depend less on the aspect ratio than on the minimum feature size. From these images, a feature size of 200 μm seems to be the minimum acceptable range for this printer. A further test was needed to measure the yield of such high-aspect ratio tests.

Pillar Test

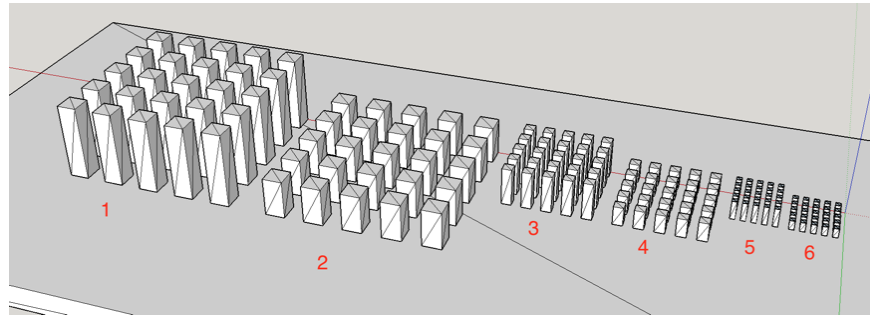
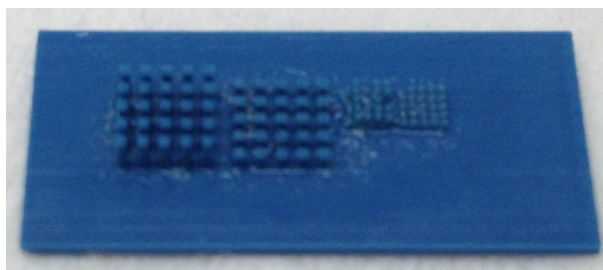


Figure 7: CAD model for pillars test. Various aspect ratios were tested for yield.



Structure Index	Pillar Dimensions (w, h) (mm)	Aspect Ratio	Yield
1	0.4, 1.6	4.0	100%
2	0.4, 0.8	2.0	100%
3	0.2, 0.8	4.0	68%
4	0.2, 0.4	2.0	72%
5	0.1, 0.4	4.0	0%
6	0.1, 0.2	2.0	0%

Figure 8: Results of pillar characterization test. Yield seems to depend more on the minimum feature size than aspect ratio (as long as aspect ratios are below 4). Structure with dimensions below $100\ \mu\text{m}$ did not print.

The pillar test validated our suspicion that the quality of the print depended less on aspect ratio than on minimum feature size. Again, anything below $100\ \mu\text{m}$ would not print and $200\ \mu\text{m}$ thick pillars had a yield of about two thirds, where most of the destroyed pillars were neighboring another section of the print. See Figure 9 for optical images.

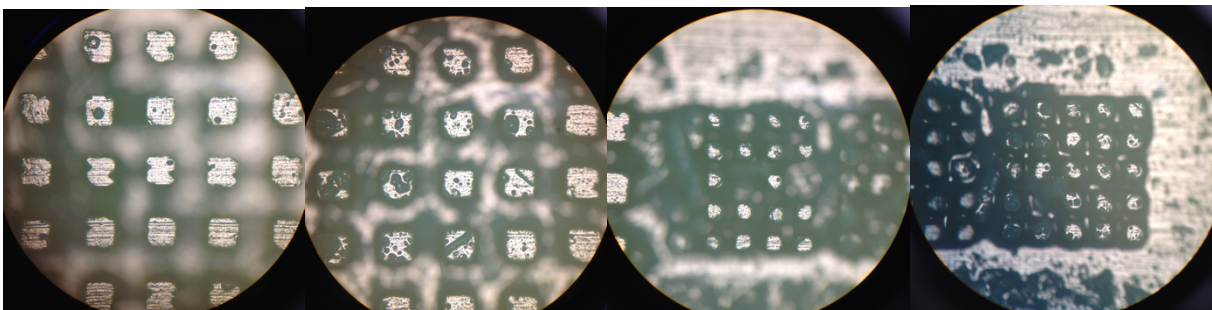


Figure 9: Optical images of pillar test results.

Well Test

Finally, a well test was printed to measure the ability of the printer to reconstruct small channels and the post-processing to successfully remove all support material. In order to fully remove support material, ultrasound was a great benefit. Light ultrasound (80kHz, 40% power, 30 sec on ExFab machine) was used to remove deep pits of support material wax after post-

processing. If there were small hanging structures, however, these would be destroyed by this exposure to ultrasound, so a balance must be made.

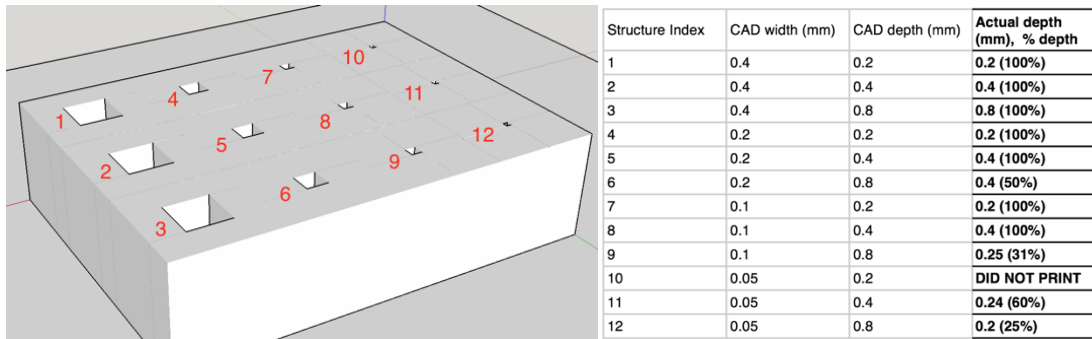


Figure 10: CAD model, dimensions, and depth measurements for well test characterization print. A variety of well widths and depths were printed to test the ability of our procedure to remove support material and faithfully replicate this model. Well depth was tested by measuring the change in focal distance to focus on the bottom of each well.

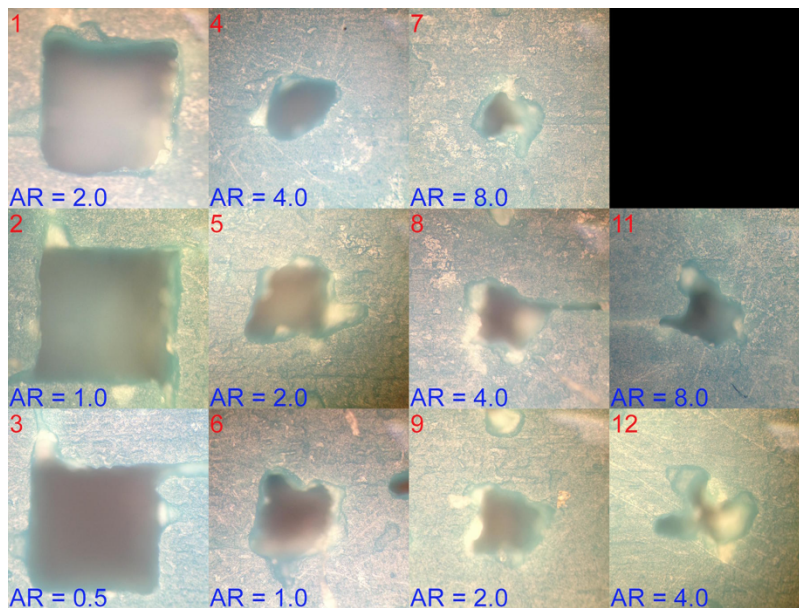


Figure 11: Optical images of well tests with a variety of aspect ratios. All images are on the same scale.

Optical images show that the printer was able to print wells much smaller than the minimum printable feature size of 200 μm . 50 μm wells were printed successfully, although it is unlikely that the resulting channel would be printed past an aspect ratio of 4.

After compiling notes on the printing and post-processing procedure, we accumulated a list of the most common sources of error that could result in poor print quality. These errors are listed in order of importance.

Sources of Error

Below is a list of possible sources of error that the 3D printing process can create, and what solution, if any, can be done to fix them:

Inability to print features 100 micron thickness or below

When we attempted to print channels 100 microns thick or less, the features simply would not print, although one the 100 μm width grid on the screening test did barely print. We hypothesize that the advertised resolution of 6 μm on this tool describes the resolution of small features on larger structures (e.g. decorations on a ring). After all, the printer is primarily used for jewelry. Some examples of failed print jobs with thin features are shown below:

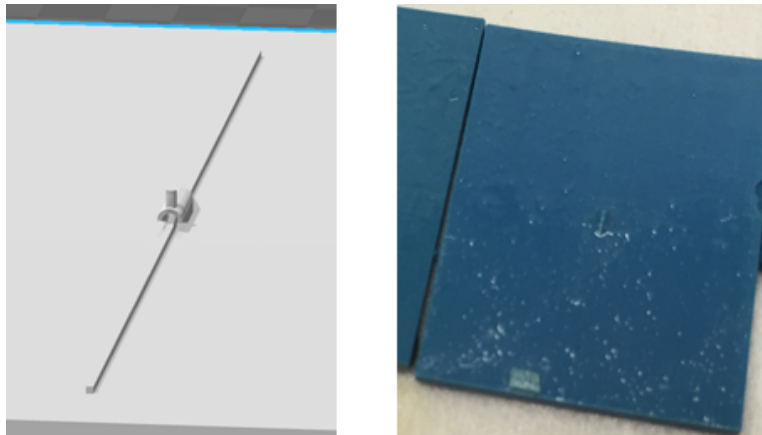


Figure 12: STL file (left) and final print (right) of a channel with many features less than 100 microns. Few of these features printed.

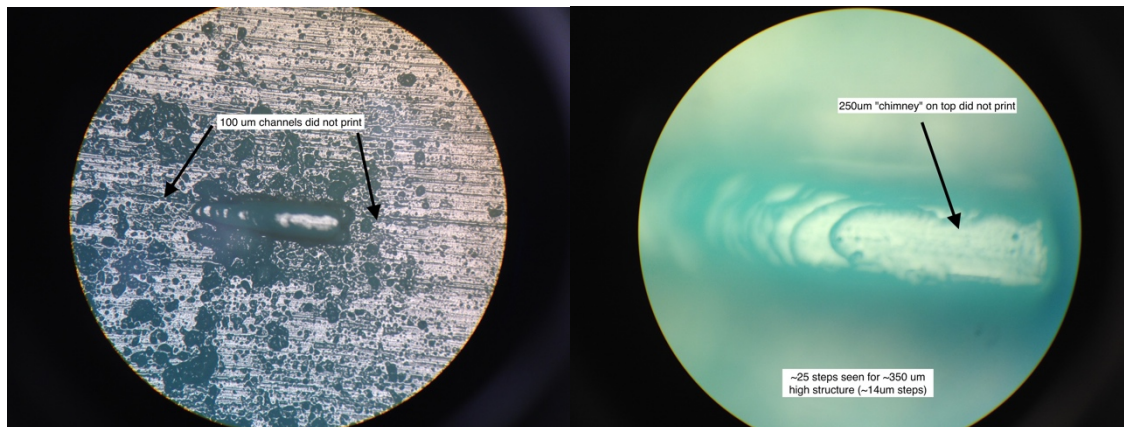


Figure 13: Optical images of the same 100 μm channel device. The channels did not print and a layer height of $\sim 14 \mu\text{m}$ was approximated by counting the steps in the right image. The 250 μm "chimney" on top of the device also did not print.

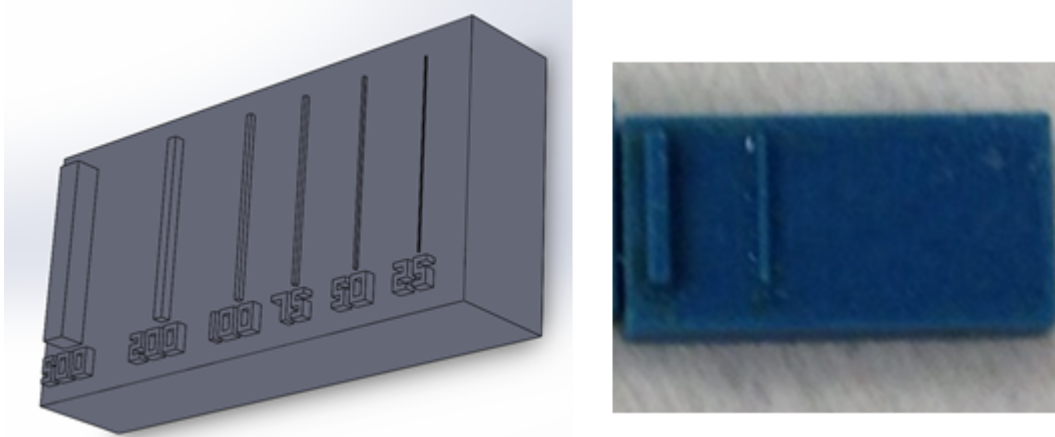


Figure 14: STL file (left) and print (right) of a characterization print of channel thicknesses. Only the 500 μm and 200 μm channel were printed.

Breakage due to rough handling

Right after printing molds, they must be removed from the build plate. The printer prints a layer of supporting “red” wax to the bottom of each print which must be heated to free the print from the build plate. To do this, the build plate is placed on a hot plate heated to 110 degrees celsius. The molds need to be gently scraped off so as to not damage any features. This scraping process can lead to snapping, cracking, or other mechanical damage. Pictures of the molds attached to the build plate, as well as possible damage that can ensue, are shown below:

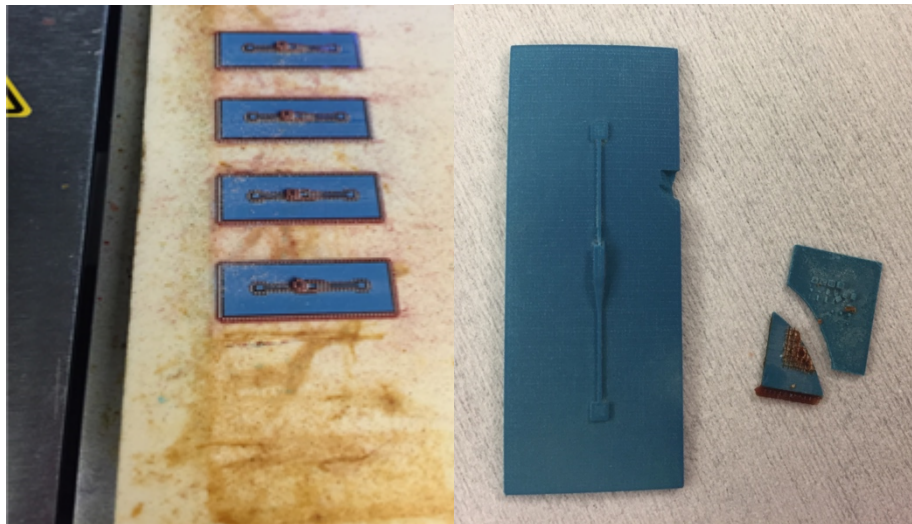


Figure 15: (Left) molds stuck to the build plate before scraping. (Right) Molds that have been chipped or snapped by improper handling

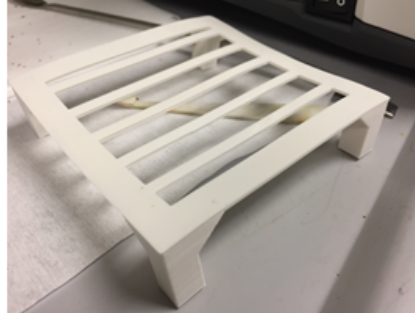
Warping

During post processing, the molds are submerged in a heated mineral oil bath to remove the support wax from the build material. If the molds are left in the bath too long, overheating can lead to warping, as shown in the figure below. There are two ways to prevent warping. Firstly, care must be taken to make sure that the molds are not submerged in the bath for more

than an hour and a half. Secondly, it is important not to let molds touch the floor of the beaker, which conducts heat from the hot plate much more quickly than the mineral oil bath. To solve this, a 3D printed plastic table was built to suspend molds in the bath. A picture of warping, along with the table, are shown below.



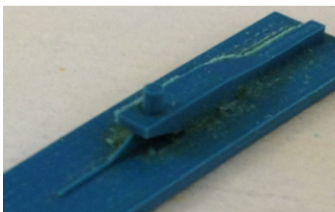
Warping of a mold improperly post-processed.



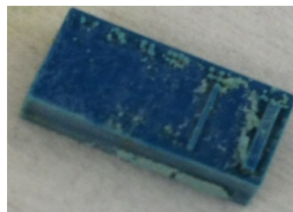
The 3d printed table used to support the molds. Warping of this table (made with PLA) also occurred.

Residue

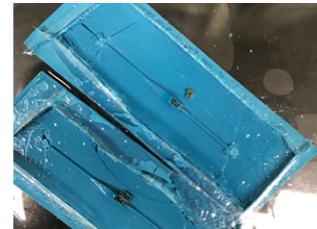
Several different types of residue can accumulate on the molds if processed incorrectly. Different observations of residues are shown in the images below:



Leftover red wax



Build material residue



Leftover red wax.

The first image of residue results when the molds are submerged for too long in a bath that isn't hot enough. This residue is difficult to remove. To avoid the buildup of this residue, it is important to use a thermometer to constantly monitor the temperature of the bath.

The build material residue results from dust created during printing. During printing, powder can build up on the molds if the vacuum bag attached to the printer is not changed properly or frequently enough. Once the molds are submerged in the bath, this dust doesn't float away. Instead, the mineral oil clumps the dust together, which sticks to the surface of the mold. Once the mold dries, the clumps remain, forming the blue residue. If the structure is stable enough, this residue can be gently scraped away using a napkin or some sort of sharp edge. There is no better way to remove this residue that we know of. Brushing away any small dust particles before submerging the molds in the bath is another good preventive measure.

Finally, leftover red wax can remain even after the molds are submerged in a heated bath for a full hour and a half. This happens more so if there are long, narrow channels that the mineral oil bath cannot easily dissolve. To remedy this issue, the molds can be removed from the mineral oil bath after about an hour or so. After one more hour of cooling, they can be safely placed back into the bath for another hour. Two hours of bathing should sufficiently remove all the wax.

Sheath Flow Device Design and Fabrication

Device Design

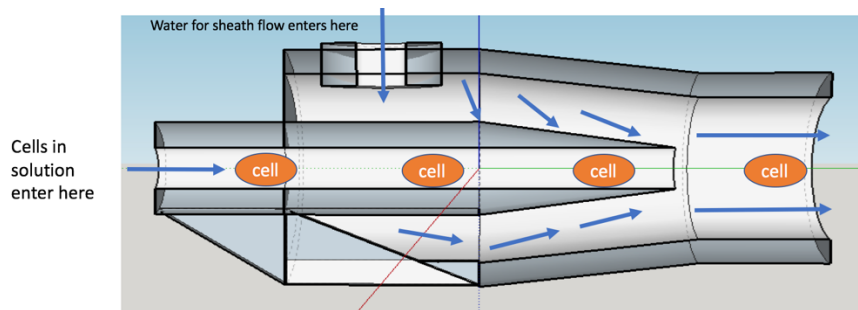


Figure 16: Ideal radial design for sheath flow. This would not be directly printed, but instead its negative would be printed as a mold for PDMS.

Our ideal design features a nozzle within a nozzle: sheath flow would surround a central flow oriented by a suspended channel. In order to print this device on small scales, a simpler, rectangular design was adopted for proof of principle.

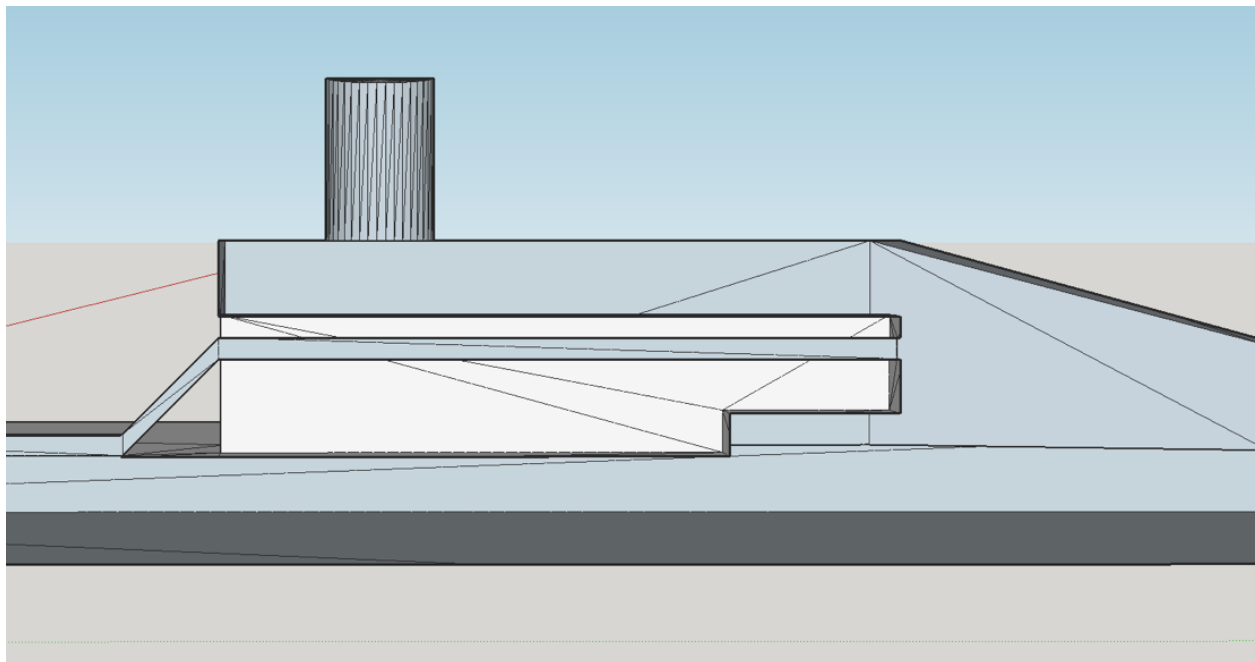


Figure 17: Mold design for a more practical iteration. Rectangular features are easier to print precisely on the smallest scale of the printer. In order to print the inverse of the channel as a mold, we designed our device by drawing the desired flow of the fluids.

In our design of the central channel we faced various trade-offs. Increasing the length of the central channel without supports would improve the uniformity of the sheath flow, but the central channel would then be very weak (especially if molded using PDMS). Also, increasing the length of the inner channel would create a longer crevice for the support wax to melt out of during mold post-processing. There are two lengths to consider under the inner channel: one is

the length of the wax mold's channel and the other is the length of the gap beneath the channel. The gap below the channel will correspond to PDMS and the length of wax will constitute the inner flow. Both the wax's channel and the PDMS gap underneath should be large enough to support itself during all steps of fabrication without breaking. The design was iterated until a happy medium was found in the designs below.

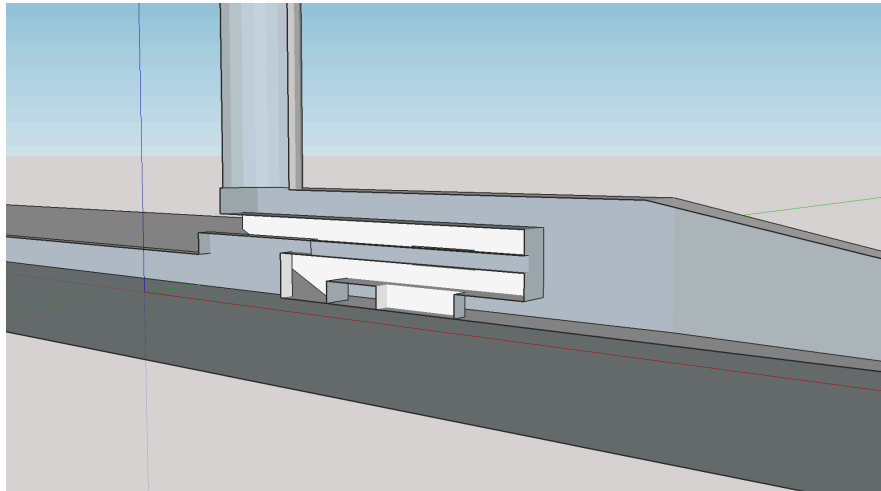


Figure 18: Slice of final square design. Gaps in the bottom support material provide space for sheath fluid to move around the central channel. The central channel's thickness was increased to provide more PDMS support. The upper chimney was lengthened to allow a direct tubing connection to the fluidics setup without cutting a hole in the PDMS.

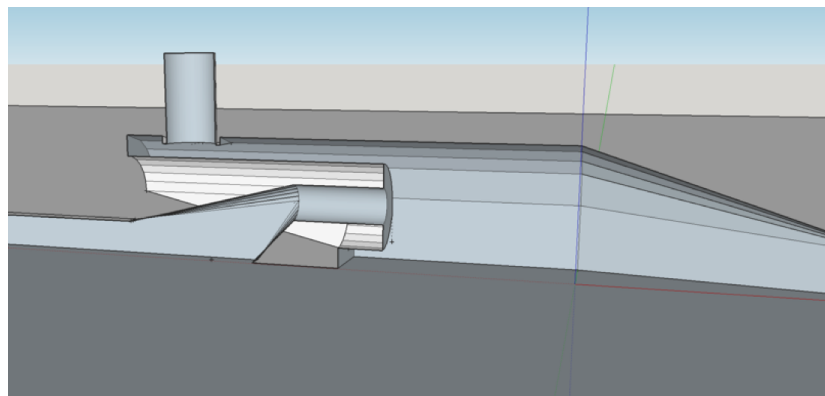


Figure 19: Slice of final radial design.

Design files (including those for characterization) are included on the wiki along with the printer's equipment page.

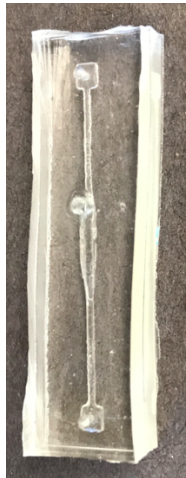
Choice of Materials

For the fabrication of microfluidic channels, we tried PDMS and many different types of epoxy as shown in Table 1.

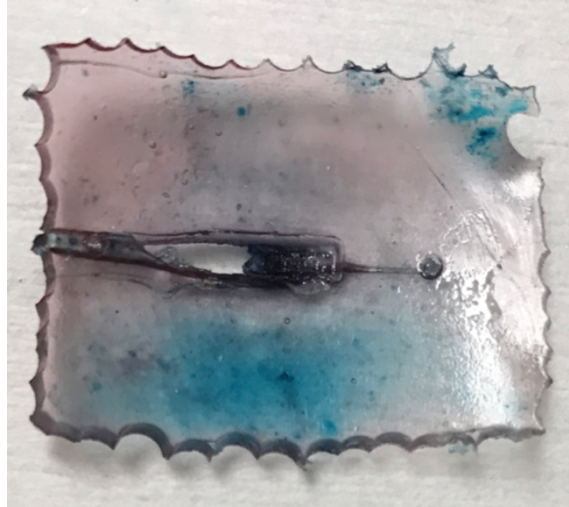
Table 2: Fabrication materials and properties

Materials	Description	Vendor	Uncured mixed viscosity (cps)	Tensile strength (MPa)	Young's modulus	Working time	Curing time and condition	Color
PDMS	Polydimethylsiloxane, prototyping polymer	Dow Corning	5550	2.2	360-870 kPa	NA	~2 hrs (@65°C)	Clear
Conapox y FR-1080	High temperature epoxy	Cytec Industries	2500	29	2.7 GPa	>2 hrs	4-16 hrs (@120°C)	Light amber
5-Minute Epoxy	Rapid-curing epoxy	Devcon Devcon	10000	13	1.2 GPa	3-6 mins	0.75-1 hrs	
2-Ton Epoxy			8000	16	1.5 GPa	30-35 mins	~2 hrs	
SU-8 3005	Epoxy-based negative photoresist	MicroChem	70	60-75	2.0 GPa	NA	100-350 mJ/cm ² UV radiation (exposure energy depends on thickness)	
SU-8 2025			5485					
SU-8 2075			27192					
SU-8 5			338					
SU-8 100			60000					

Because the melting point of wax is 95-110 °C, the wax mold will melt at the high temperature epoxy's curing temperature. As summarized in Table 2, PDMS is soft, clear, and widely used for the fabrication and prototyping of microfluidic chips. However, the flexibility of PDMS does not make it ideal for strong 3D-molded structures, especially for suspended structures like our inner channel. Epoxy is hard and strong enough for 3D structure, but it must be of a low enough viscosity so that bubbles do not form around small features in the mold. In order to tweak the mechanical properties of epoxy, we tried adding organic solvent, such as ethanol, to decrease the stiffness and increase curing time for bubble removal, but as most organic solvents can dissolve wax mold this method destroyed our mold. Another option is photocurable epoxy, SU-8. Since the curing of SU-8 is caused by radiation and not time, bubbles can be removed well before curing increases its viscosity. However, epoxy will distort slightly after it is heated above 100°C. In addition, epoxy is difficult to bond to PDMS without using a clamp or epoxy glue.



PDMS channel



Distorted epoxy channel

Table 3 Advantage and disadvantage of fabrication materials

Material	Pros	Cons
PDMS	Soft Clear Easy to bond Thermostability	Too flexible for some 3D structures
Rapid-curing epoxy	Strong 3D structure Short curing time	Hard Fragile Bubble Wax removal problem Distorted when heating to 100°C Hard to bond
SU-8	Strong 3D structure Photocurable (radiation curing) Thermostability	Expensive (relatively) Bubble Hard to bond

Based on the advantage and disadvantage above, we choose PDMS as our fabrication material for microfluidic channels.

Microfluidic Fabrication

PDMS is poured over the wax mold and placed in a desiccator to remove bubble (it could also be centrifuged before pouring). We then put the PDMS with wax mold into 65°C oven for 4 hours to cure. After PDMS cured, we melt the wax mold out at around 140°C. The PDMS channel is then bonded to another piece of PDMS via plasma bonding.

Sheath Flow Tests

Considering the resolution of wax printer, we printed the channel design on a millimeter scale for proof of principle. The diameters of inner channel are 200-400 μm and the outer sheath flow channel is 1-2 mm at its largest. The flow rate we used was 0.05-2 mL/hr. In this condition, the maximum Reynolds number of the system is around 0.8, indicating that all the

flows in the system are laminar; the Péclet number in the system is around 64000, indicating that fluids after the nozzle will remain largely unmixed.

The fine inner channel of the device was very fragile. It could easily be broken and it hardly allowed enough flow rate for inner flow. Based on the results, we redesigned the channel several times, ending up with a radial one with wider inner channel and stronger support (Figure 19). This design, although bad for sheath flow uniformity, had the structural support to produce consistent results.

During test, we flowed two fluids with different food dye into the channels. As shown in Figure 20, fluids inside channel keep laminar, and sheath flow is formed in vertical direction. However, we did not see radial sheath flow. One possible reason is that the diameter of the sheath flow channel is still much larger than that of inner channel. The difference in diameter caused a difference in velocities and the fluids' behavior as a consequence. In addition, the sheath flow probably needs a longer channel to be stable and symmetric before mixing.

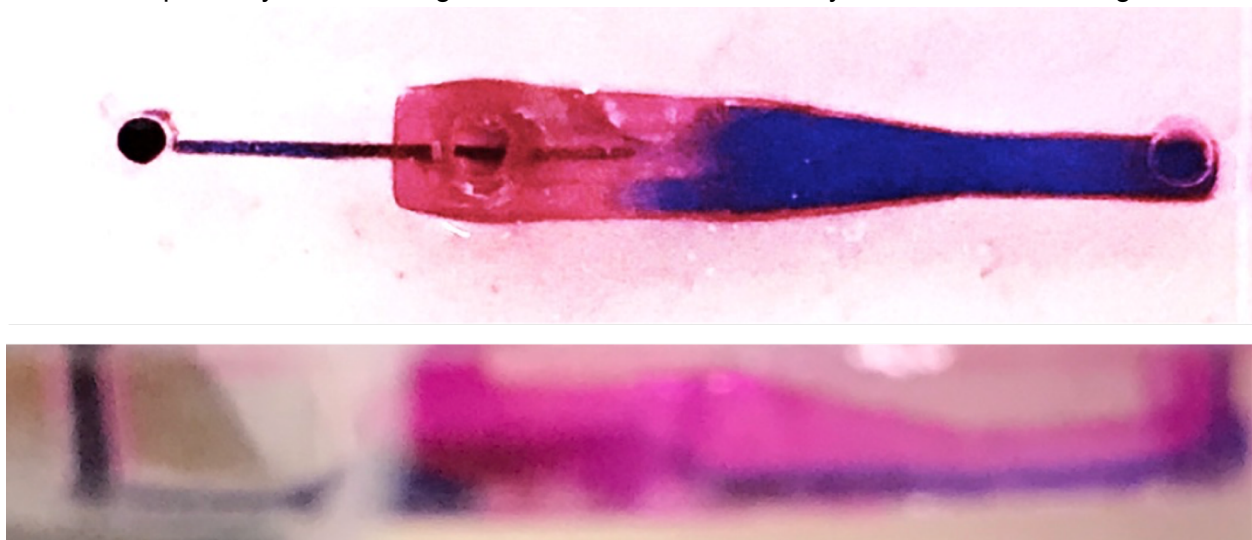


Figure 20: Top view and side view of channel with fluids inside.

To improve our results, we propose adding more symmetric support for the suspended channel, decreasing the channel diameter and flow rate of sheath flow, and increasing the channel length.

Conclusion

Using wax printer, we can easily fabricate a 3D microfluidic channel overnight, while traditional microfluidic channel fabrication using photolithograph needs much longer time (~1 week) and can only give 2D structures. However, the resolution of wax printer (~200 μm) is not competitive with the resolution of photolithograph (~5 μm). Also, it is easy to print several wax molds at the same time but each wax mold is necessarily disposable, while the master fabricated by photolithography can be used multiple times. We found that printing multiple copies of the same design was time consuming but necessary for process development.

Table 4 Comparison of traditional microfluidic channel fabrication and our method

Traditional microfluidic channel fabrication	Our method using 3D wax printer
<ul style="list-style-type: none">• Time-consuming (~1 week)• 2D (stacking for “2D+”) structure• Multi-time use of master• High resolution (~5 μm)	<ul style="list-style-type: none">• Rapid (~1 day)• 3D structure• One-time use of wax mold• Low resolution (~200 μm)

Future work to improve our results would benefit from microfluidic simulations using our model geometries and process development for creating epoxy molds that do not deform under heat.

Appendix – Further Documentation and Code

Preparing and Loading Molds into Wax Printer

A detailed procedure for creating wax molds with this specific tool is uploaded to the wiki.

Post-Processing Procedure for Wax Molds

A video is available online showing the wax mold removal process:

<https://youtu.be/6ClhzsoEYZQ>

3d Model Automation Scripts

In order to automate the creation of 3d stl files for printing characterization tests, supporting Python scripts were developed for developing and scaling stl files. Automatic scripts for iterating multiple aspect ratio dimensions, for example, saved a lot of time. Also, the CAD software used often could not support the creation of basic shapes at the desired dimension, requiring the user to create the desired geometries at a larger scale. Scaling the files was useful for taking existing complicated models (e.g. designed in Google SketchUp or Solidworks) and scaling them down to the desired dimension. See <https://github.com/rexgarland/stl-utilities> for this code and its documentation.

References

[1] Hofmann, Oliver, Philippe Niedermann, and Andreas Manz. “Modular Approach to Fabrication of Three-Dimensional Microchannel Systems in PDMS—application to Sheath Flow Microchips.” *Lab Chip* 1, no. 2 (2001): 108–14. doi:10.1039/B105110P

[2] Rekštytė, Sima, Mangirdas Malinauskas, and Saulius Juodkazis. “Three-Dimensional Laser Micro-Sculpturing of Silicone: Towards Bio-Compatible Scaffolds.” *Optics Express* 21, no. 14 (July 15, 2013): 17028. doi:10.1364/OE.21.017028.